Adipose-derived mesenchymal stem cells secreted EVs: a potential cell-free therapy for canine renal ischemia-reperfusion injury

Hai-Feng Liu
Sichuan Agricultural University
Chen Fuhao
Sichuan Agricultural University
Huang Liyuan
Sichuan Agricultural University
Cao Jiahui
Sichuan Agricultural University
Liu Yifan
Sichuan Agricultural University
Zhong Zhijun
Sichuan Agricultural University
Zhou Ziyao
Sichuan Agricultural University
Ren Zhihua
Sichuan Agricultural University
Cao Suizhong
Sichuan Agricultural University
Shen Liuhong
Sichuan Agricultural University
Peng Guangneng (Pgn.sicau@163.com)
Sichuan Agricultural University
Ma Xiaoping
Sichuan Agricultural University

Research Article

Keywords:

Posted Date: June 24th, 2022

DOI: https://doi.org/10.21203/rs.3.rs-1774426/v1

Abstract

Canine renal ischemia-reperfusion (IR) causes severe acute kidney injury characterized by renal dysfunction and inflammatory disorder. Adipose-derived mesenchymal stem cells (ADMSCs) and their extracellular vesicles (EVs) are pluripotent adult stem cells with promising therapy for IR, based on their potent anti-inflammatory and immunomodulatory properties. The aims of this study were to explore the therapeutic efficacy of ADMSC-EVs in canine renal IR injury. MSCs were isolated from inguinal fat tissue in dogs and their EVs were isolated from third-passage of ADMSC. ADMSCs were charactered by differentiation ability and surface makers. ADMSC-EVs were charactered by transmission electron microscopy, NTA and surface markers. Canine IR model was used with ADMSC-EVs administration to evaluated the therapeutic effect of inflammation, oxidate stress, mitochondrial damage and apoptosis. Renal IR injury leads to severe histopathological lesions and significantly increasing in biomarkers of renal function, inflammation, apoptosis; however, ADMSC more potently attenuated these lesions and inhibited apoptosis by reducing mitochondrial damage. The findings may provide a cell-free therapy for canine renal IR injury and reveal the mechanism involved.

Introduction

Over the past decade, stem cell therapy showed potential in regenerative medicine therapies for multiple diseases. Mesenchymal stem cells (MSCs) have emerged as a promising cell-based therapy for acute kidney injury (AKI) (M. Huang et al., 2022). The mechanism of MSC therapy for IR injury may involve macrophage polarization, NF-κB and TGF signal pathway activating (C. Huang et al., 2022; Zhang et al., 2022).

Recent studies have shown that MSC exert their effects not through differentiation(Enam, Kader, Bodkin, Lyon, & Bellamkonda, 2020). MSC will be eliminated soon via monocytes and macrophages(de Witte et al., 2018; Galleu et al., 2017). A further mechanism whereby short-lived MSC could mediate prolonged disease-modulated effects is through the release of extracellular vesicles (EV) – lipid-bilayer-enclosed subcellular particles that contain a “cargo” of bioactive molecules and participate in cell-cell communication. In particular, the small size of EV (30–120 nm) compared to intact MSC (30 μm) may allow them to avoid entrapment in the lungs and be rapidly distributed systemically and internalized by immune and epithelial cells within the kidneys(Fazekas & Griffin, 2020).

Renal IR is most common induction of renal disease including renal failure and nephritis clinical in both human and animals. Usually, it is inevitable of renal IR in routine circumstances or surgery. Our pilot study showed renal lesion occurred immediately after renal ischemia reperfusion and reach the maximum at 30h post-operation. Accompanying with oxygen radical produced, mitochondrial dysfunction, inflammations, organs with IR injury leads to a series histopathological changes of adhesion molecules enhanced, activation and infiltration of macrophages and neutral granulocytes which was related with the release of inflammatory cytokines (Pefanis, Ierino, Murphy, & Cowan, 2019).

Some therapeutic measures such as pre-ischemia, antioxidants, adrenoceptor agonist (dexmedetomidine), sulodexide, hydrogen -rich water were used to prevent or attenuate the impact of IR and received efficacious effect (Li et al., 2018; Yin et al., 2017). While the studies of MSC showed stupendous therapy potential of organ injury due to the function of anti-inflammatory and immunomodulatory. The function was mostly induced by paracrine system including extracellular vesicles (Lerman, 2021). Researchers proposed the hypothesis that combined application of ADMSCs and its extracellular vesicles may be a satisfied therapeutic treatment for acute renal injury(Lin et al., 2016).

The objective of this study was to evaluated the ability of ADMSC-EVs in renal ischemia-reperfusion injury. We identified the characteristic of canine ADMSC and their EVs, explored the effect of ADMSC-EVs in recovery of renal function and anti-apoptosis. We further explored the treatment efficacy of ADMSC-EVs transplantation in canine IR -AKI model.

Materials And Methods

Beagles aged 10–12 months were used in the study. The dogs were kept under circadian rhythm and had free access to food and water. The dogs were obtained from Qionglai animal farm (ChengDu, China). The experimental protocol was approved by the Sichuan Agricultural University Ethical Committee (China). Care and handling of the animals were performed in accordance with the Guide for the Care and Use of Laboratory Animals published by the National Academy Press (National Institutes of Health Publication No. 85 − 23, revised 1996).

ADMSCs isolation, characterization, and culture

Under anesthesia, inguinal fat (about 5g) was collected for MSC extraction procedure. After type Ⅱ collagenase (Beijing Suolaibao Technology Co., Ltd. Beijing, China) digestion, filter, centrifugal sedimentation, ADMSCs were isolated from inguinal fat tissue in dogs and cultured(Bukowska et al., 2021) with complete culture medium supplemented with 10% EQ-FBS in 37℃ and 5% CO_2. Then cells ($2.0–6.0×10^6$/mL) were characterized based on the expression of common MSC markers (CD34, CD29, CD45, CD105, ITGB and CD90) (Huang et al., 2021) followed flow cytometry (CytoFLEXS, DAPI, Hoechst Blue, Germany) of the third-passage of ADMSC.

Induction of MSC differentiate

ADMSCs of passage 3 (P3) cells were inoculated in 6-well cell culture plates at a density of $4×10^3$ cells/cm^2. To determine the differentiation ability of MSC, the culture medium in the hole was removed, and 2 mL osteogenic medium (Cyagen) or lipogenic medium (Cyagen) was added to each well of the experimental group for changing the medium every 2 or 3 days. Adipocytes were stained with oil red O after 14 days of lipogenic differentiation induction, and osteocytes were stained with alizarin red after 21 days of osteogenic differentiation induction for identification.

EVs isolation and characterization

EVs were isolated from supernatants of ADMSCs (5×10^6) by ultracentrifugation. Sequent, the concentrated solution was enriched by supernatant centrifugation via sucrose density gradient from the supernatants as previously described(Kholia, Sanchez, Cedrino, Papadimitriou, & Camussi, 2018; Ling et al., 2018). The prepared sucrose solution and concentrated solution were successively added to the ultracentrifugation tube in a ratio of 1:8, and centrifuged 110000 g at 4℃ for 70 min to collect the heavy water layer. Appropriate PBS was added for re-suspension, and centrifuged 110000g at 4℃ for 70 min again to collect precipitation, which collected precipitates were suspended in 50 ~ 100μL PBS.

EVs were characterized by typical marker proteins and the protein concentration was detected via BCA (Beijing Solarbio Science & Technology Co.,Ltd.). Morphological structure was observed via transmission electron microscopy, and particle size distribution was analyzed via NTA. Surface markers including exosomal markers (CD63, CD9, Tsg101) were analyzed by western blotting.

Animal models and therapeutic experiments

After adaptive feeding for a week, 12 beagles that were normal after physical examination, blood routine examination and kidney b-ultrasound screening were numbered. They were divided into 4 groups randomly: blank group (operations with left kidney exposure but without renal vessels clamping and right nephrectomy, n = 5), model group (operations with left renal vessels clamping and right nephrectomy, n = 5), control group (administration PBS in IR model, n = 5) and experimental group (administration EVs in IR model, n = 5). There was no significant difference in body weight between groups.

After the induction of Zolazepam, teletamine and propofol, all the experimental dogs could maintain anesthesia by isoflurane inhalation. The left renal vessels were separated through the incision of ventral midline and the renal arteries and veins were clipped with noninvasive hemostatic clip (5.7 cm, Shanghai Medical Instrument Co. Ltd. China) for 60 min to induce ischemia injury, and reperfusion injury was induced after the clip was released. The kidneys were monitored by a color change to confirm blood reflow. Right nephrectomy was performed immediately after the clip released. Physiological saline was affused into the abdominal cavity for lavage. The incision was then sutured routinely.

After the clip released, the left kidney was injected with EVs (180μg/kg) in renal cortex for experimental group, while PBS was injected for control group. Serum samples were collected and stored at -80℃ for further analysis after reperfusion 3h, 6h, 12h, 24h, and 30h. After reperfusion 30h, kidney tissue samples were collected laparotomy.

Sterile instruments were used for all procedures. All surgical procedures were performed by the same trained surgeons in same environment.

H&E staining, TUNEL, and TEM

Renal tissue was collected from the caudal pole of left kidney. The renal tissue was fixed in 10% buffered formalin, embedded in paraffin, and sliced in 3 μm-thick sections. Sections were stained with HE (haematoxylin-eosin) to evaluate histopathological change. Five pictures of each sample were analyzed to compare changes among different timepoints after surgery. Ten fields were randomly selected at 200 times, and 10 renal tubules were scored in each field whose degree of renal tubule injury adopted for Paller scoring standard(Paller, Hoidal, & Ferris, 1984).

Renal tissue was paraffin embedded for immunofluorescence staining of TUNEL to observe the apoptosis of kidney cells, which a bit of renal cortex was fixed in electron microscope fixative at 4℃ and stored away from light for TEM (HITACHI, H-7560, Japan) to observe mitochondrial structure.

ELISA

Serum concentration of IL-1β, IL-10, IL-6, TNF-α, Cystatin C in the previous collected samples and the activity of SOD, MPO, the concentration of MDA in renal tissue was detected used ELISA kits (R&D Systems, Inc, Minneapolis, Minnesota, USA). The concentration of SCr and BUN in serum were determined by automatic animal biochemical analyzer (Catalyst One, IDEXX, USA).

Statistical analysis

All data were analyzed using SPSS 20.0 software for one-way ANOVA and t-test. The results were expressed as mean ± standard deviation (mean ± SD) and P□0.1 indicates significant difference. All charts were plotted using GraphPad Prism 7 software.

Result

Isolation, and Characterization of ADMSC

ADMSC was cultured successfully after passage 4 and the morphology was observed under an inverted microscope. ADMSC were cultured in 24 posterior adherent cells. The primary ADMSCs were cultured for 2–4 days and the cells were spindle-shaped and polygonal. The cells reached 80% confluence in culture after 4–5 days. ADMSCs exhibited the morphologies of fusiform and typical spindle shaped at passage 3 (Fig. 1A, B).

Differentiation of ADMSC

ADMSC inducted with adipocytes and osteocytes exhibit the differentiation ability with lipogenic and osteogenic. After 21 days of culture in induction medium, lipid droplets had formed in the induced ADMSCs(Fig. 1C). Alizarin-red staining was positive as calcium nodules after 21 days of induction (Fig. 1D).

To identify the MSCs isolated, we detected the surface markers (CD45, CD34, CD31 CD105, CD90, ITGB) from cells of passage 3 by flow cytometry. Result showed that surface markers including CD45, CD34,

CD31 exhibited 1.65%, 0.94%, 3.77% positivity respectively;and markers including CD105, CD90, ITGB exhibited 97.8%, 98.45%, 85.32% positivity respectively (Fig. 1E).

Isolation, and Characterization of ADMSC-Evs

EVs morphology of the four groups was observed by transmission electron microscopy (Fig. 2A). EVs exhibited the characteristic cup-shape morphology, and were within the normal vesicle size range (30–150 nm in diameter). The number and average size of EVs was measured via NTA, which turned out as 9.7×10^{9}/ml and 134 nm (Fig. 2B). The protein content of ADMSC-EVs was measured to be 0.36 ug/ul via ultramicro spectrophotometer. Extracellular marker (CD63, CD9) and intramembrane marker (TSG101) were detected positively via western blot (Figure C)

MSC-EVs protect against renal I/R injury in canine

Renal IR resulted in markedly elevated levels of renal function biomarkers (serum creatinine, BUN, Cys-c), histopathological changes, subcellular structure and apoptosis, inflammation biomarkers (TNF-α, IL-6, IL-1β, IL-10), oxidative stress (SOD, MPO, MDA), whereas these injury parameters were ameliorated by MSC-EVs treatment.

The serum concentration of Scr, BUN increased postoperatively and continuous increased to 30h, the serum concentration of Cys-c increased postoperatively, and started to decrease after 24h in all groups. After ADMSC-EVs were injected into the cortex, the serum concentration of Scr, BUN was lower significantly after 24h postoperatively and the serum concentration of Cys-c was lower significantly after 12h postoperatively comparing with the control group (Fig. 3A).

The serum concentration of TNF-α, IL-6, IL-1β, IL-10 increased postoperatively, and started to decrease after 12h. After ADMSC-EVs were injected into the cortex, the serum concentration of TNF-α, IL-6 was lower significantly after 3h postoperatively and the serum concentration of IL-10 was lower significantly after 6h postoperatively comparing with the control group (Fig. 3B).

Histopathological changes showed that severely lesions emerged in renal IRI including tubular dilation, epithelial cell swelling, mild granular degeneration, nuclear pyknosis, cellular cast, inflammatory cells infiltrating in renal interstitium. Administration of ADMSC-EVs relieved this situation including tubular dilation, epithelial cell swelling, mild granular degeneration, cellular cast, inflammatory cells infiltrating in renal interstitium in experimental group (Fig. 4A). The application of ADMSC-EVs alleviated renal lesion caused by IR by way of Paller score (Fig. 4B).

The serum concentration of MDA and MPO activity increased at 30h postoperative, and decreased to normal level when ADMSC-EVs was administrated. The serum concentration of SOD decreased at 30h postoperative, and increased to normal level when ADMSC-EVs was administrated (Fig. 4C).

The results showed that the apoptotic rate in model group was significantly higher than that in blank group. Whereas the apoptotic rate in experimental group was lower compared with that in model group

(Fig. 4D).

We evaluated the effect of renal IR on mitochondrial morphology, which is indicative of apparent mitochondrial damage (Fig. 4A). Renal IR induced a reduction in the number of mitochondrial and larger of single mitochondrial. Reduced mitochondrial matrix particles, shorten or reduced cristae, part of dissolved mitochondrial matrix and cavitated mitochondrial was also observed in model group. EVs from ADMSCs reversed the quantity and morpho of damaged mitochondrial somewhat.

Discussion

Due to similar organ morphology and structure, canines were used as disease model in the field of biology and medicine (Amorim et al., 2020; Matta et al., 2022). MSC derived from adipose, placenta and marrow possess the potential to attenuate multiple diseases(Han et al., 2022). The dog has been used to evaluate MSC therapy for the treatment of several inflammatory conditions including osteoarthritis, spinal cord injury, inflammatory bowel disease, and graft-versus-host disease(Fazekas & Griffin, 2020). It is the standard procedures that MSCs should be identified with surface biomarkers and the capacity to differentiate and their extracellular vesicles should be identified with transmission electron, NTA, extracellular marker (CD63, CD9), intramembrane marker (TSG101)(Dominici et al., 2006; Nieuwland, Falcon-Perez, Thery, & Witwer, 2020).

EVs derived from MSC exhibited potential as cell-free therapies for organ injury, tumor suppression and immune response regulated in various animals. Riazifar M et al. found that MSC-EVs created a tolerogenic immune response to treat autoimmune and central nervous system disorders, decrease neuroinflammation and demyelination with experimental autoimmune encephalomyelitis by inhibiting the immune capacity of mice(Riazifar et al., 2019). Furthermore, there is increasing evidence that ADMSC-EVs derived stem cell play a positive role in attenuating or preventing AKI(Aghajani Nargesi, Lerman, & Eirin, 2017). Based on the above results, the current study investigates the hypothesis that ADMSC-EVs can protect the kidneys against canine renal IRI. Additionally, this study demonstrates that treatment with ADMSC-EVs inhibits renal cell apoptosis, mitochondrial damage, and production of peroxide, which preserves kidney structure.

IRI contributes to the stimulation of histopathological damage for the renal tissues. Severe infiltration of focal inflammatory cells was observed in the cortex between the degenerated tubules in rats with renal IRI. In addition, the corticomedullary portion also showed degeneration in the lining tubular epithelium and there was periglomerular focal inflammatory cells aggregation at the cortex in the lumen of most of these tubules(M. A. Fawzy, S. A. Maher, S. M. Bakkar, M. A. El-Rehany, & M. Fathy, 2021). In our study, H&E staining reveals that the model group exhibits renal tubular swelling, vacuolization, necrosis, detachment of tubular basement membranes, while it was improved in the experimental group. In addition, the degree of renal tubule injury was evaluated by Paller's scoring standard(International, 1992), which shows ADMSC-EVs intervene renal IRI damage effectively.

The urinary protein BUN and SCR were increased in renal IRI(Q. Ling et al., 2017). Sayed Zeid AS also found that the there was a significant rise in the levels of serum and urinary Cys-C after 1 h in the IRI group(Zeid, Sayed, & Transplantation, 2020). CYSC concentration in blood was a desirable functional parameter and which reflected GFR (glomerular filtration rate). Similarly, in our study, it was significantly increased of BUN, SCR, and Cys-C in model group ($p < 0.01$ vs. blank group), all of which were attenuated by ADMSC-EVs. These data support the hypothesis that ADMSC-EVs attenuates renal IRI-induced renal function damage in vivo.

Oxidative stress plays a critical role in the pathogenesis of IRI(Dobashi et al., 2000), which is directly related to excessive ROS production in the affected tissue. The resultant excessive ROS or other free radicals can lead to a switch from aerobic to anaerobic metabolic pathway, ATP depletion, and cytosolic calcium overload, and activation of membrane phospholipid proteolytic enzyme(Panah, Ghorbanihaghjo, Argani, Zarmehri, & Ahmad, 2018). From hypoxia to normal blood supply, IRI leads to the production of a large number of ROS and reduced antioxidant capacity of cells(Martin, Gruszczyk, Beach, Murphy, & Saeb-Parsy, 2019). In this study, changes of renal peroxidase activity are evident discrepant in each group 30 h after reperfusion. After IRI (model group), the content of SOD has descended clearly. Over the left, the content of the MDA and MPO has risen up. These conditions were alleviated in the treatment group. Several studies have shown that superoxide overproduction caused by mitochondrial injury plays a key role in IRI(Chouchani et al., 2014; Chouchani et al., 2016). Our data can account for ADMSC-EVs can limitoxidative stress to maintain the mitochondrial function.

Inflammatory reaction will be triggered after IRI by MAPK signaling pathway, result in the increased of inflammatory cytokines(M. A. Fawzy, S. A. Maher, S. M. Bakkar, M. A. El-Rehany, & M. J. I. J. o. M. S. Fathy, 2021; Guo et al., 2018). Inflammatory reaction will be activated immediately once the blood flow was recovered from renal ischemia. There will be a maximum value of TNF-α, IL-6, IL-1β and IL-10 concentration in blood after 12-hour reperfusion, and then decreased gradually in this study. The expression of these inflammatory cytokines was significantly inhibited at every timepoints when ADMSC-EVs were used in the study.

IR injuries induced the production of reactive oxygen species (ROS). the relationship between mitochondria oxidative stress, ROS production and mitophagy are intimately interwoven(Su, Zhang, Gomez, Kellum, & Peng, 2022). Different types of cell death in kidney injury are related with mitochondrial damage. Significant damage of mitochondrial could result in cell death such as apoptosis, pyroptosis, ferroptosis and recent studies showed that multiple types of cell death can be observed after IR injuries(Doke & Susztak, 2022; Lu et al., 2022). The results also showed that high apoptosis rate emerged after renal IR and EVs derived from ADMSC attenuated mitochondrial damage and cell apoptosis.

Conclusion

The findings from this study demonstrate that canine adipose-derived mesenchymal stem cells derived EVs possess the potential of immunoregulatory and renal function recovery after IR, attenuated cell

apoptosis possibly by protecting the mitochondria. The study may provide a cell-free therapy for acute renal injury. Additional studies will be needed to further elucidate the mechanism of ADMSC-EVs modulate in organ injury repair and immune response.

Competing Interests and Funding

The authors declare no conflicts of interest. This study was supported by the National Natural Science Foundation of China (No. 32002353) and Natural Science Foundation of Sichuan Province (No. 22NSFSC3786).

Declarations

Competing Interests and Funding

The authors declare no conflicts of interest. This study was supported by the National Natural Science Foundation of China (No. 32002353) and Natural Science Foundation of Sichuan Province (No. 22NSFSC3786).

Author contributions

LHF, CFH, HLY performed the experiments, analyzed the data, wrote the article. CCJ and LYF collected the samples and prepared figures. ZZJ and RZH helped with the software and techniques. PGN, ZZJ and MXP initiated, designed, and supervised the project. PGN, CSZ and SLH reviewed and edited the manuscript.

References

1. Aghajani Nargesi, A., Lerman, L. O., & Eirin, A. (2017). Mesenchymal stem cell-derived extracellular vesicles for kidney repair: current status and looming challenges. Stem Cell Res Ther, *8*(1), 273. doi:10.1186/s13287-017-0727-7
2. Amorim, R. M., Clark, K. C., Walker, N. J., Kumar, P., Herout, K., Borjesson, D. L.,.. . therapy. (2020). Placenta-derived multipotent mesenchymal stromal cells: a promising potential cell-based therapy for canine inflammatory brain disease. *11*(1), 1–12.
3. Bukowska, J., Szóstek-Mioduchowska, A. Z., Kopcewicz, M., Walendzik, K., Machcińska, S., Gawrońska-Kozak, B. J. S. C. R., & Reports. (2021). Adipose-Derived Stromal/Stem Cells from Large Animal Models: from Basic to Applied Science. *17*(3), 719–738.
4. Chouchani, E. T., Pell, V. R., Gaude, E., Aksentijević, D., Sundier, S. Y., Robb, E. L.,.. . Smith, A. C. J. N. (2014). Ischaemic accumulation of succinate controls reperfusion injury through mitochondrial ROS. *515*(7527), 431–435.
5. Chouchani, E. T., Pell, V. R., James, A. M., Work, L. M., Saeb-Parsy, K., Frezza, C.,.. . Murphy, M. P. J. C. m. (2016). A unifying mechanism for mitochondrial superoxide production during ischemia-

reperfusion injury. *23*(2), 254–263.

6. de Witte, S. F., Luk, F., Sierra Parraga, J. M., Gargesha, M., Merino, A., Korevaar, S. S.,.. . Roy, D. J. s. c. (2018). Immunomodulation by therapeutic mesenchymal stromal cells (MSC) is triggered through phagocytosis of MSC by monocytic cells. *36*(4), 602–615.
7. Dobashi, K., Ghosh, B., Orak, J., Singh, I., Singh, A. J. M., & biochemistry, c. (2000). Kidney ischemia-reperfusion: modulation of antioxidant defenses. *205*(1), 1–11.
8. Doke, T., & Susztak, K. (2022). The multifaceted role of kidney tubule mitochondrial dysfunction in kidney disease development. Trends Cell Biol. doi:10.1016/j.tcb.2022.03.012
9. Dominici, M., Le Blanc, K., Mueller, I., Slaper-Cortenbach, I., Marini, F., Krause, D.,.. . Horwitz, E. (2006). Minimal criteria for defining multipotent mesenchymal stromal cells. The International Society for Cellular Therapy position statement. Cytotherapy, *8*(4), 315–317. doi:10.1080/14653240600855905
10. Enam, S. F., Kader, S. R., Bodkin, N., Lyon, J. G., & Bellamkonda, R. V. J. J. o. N. (2020). Evaluation of M2-like macrophage enrichment after diffuse traumatic brain injury through transient interleukin-4 expression from engineered mesenchymal stromal cells. *17*(1).
11. Fawzy, M. A., Maher, S. A., Bakkar, S. M., El-Rehany, M. A., & Fathy, M. (2021). Pantoprazole Attenuates MAPK (ERK1/2, JNK, p38)-NF-kappaB and Apoptosis Signaling Pathways after Renal Ischemia/Reperfusion Injury in Rats. Int J Mol Sci, *22*(19). doi:10.3390/ijms221910669
12. Fawzy, M. A., Maher, S. A., Bakkar, S. M., El-Rehany, M. A., & Fathy, M. J. I. J. o. M. S. (2021). Pantoprazole Attenuates MAPK (ERK1/2, JNK, p38)–NF-κB and Apoptosis Signaling Pathways after Renal Ischemia/Reperfusion Injury in Rats. *22*(19), 10669.
13. Fazekas, B., & Griffin, M. D. (2020). Mesenchymal stromal cell-based therapies for acute kidney injury: progress in the last decade. Kidney Int, *97*(6), 1130–1140. doi:10.1016/j.kint.2019.12.019
14. Galleu, A., Riffo-Vasquez, Y., Trento, C., Lomas, C., Dolcetti, L., Cheung, T. S.,.. . Dazzi, F. (2017). Apoptosis in mesenchymal stromal cells induces in vivo recipient-mediated immunomodulation. Sci Transl Med, *9*(416). doi:10.1126/scitranslmed.aam7828
15. Guo, X., Jiang, H., Chen, J., Zhang, B.-F., Hu, Q., Yang, S.,.. . Zhang, J. J. I. J. o. M. M. (2018). RP105 ameliorates hypoxia/reoxygenation injury in cardiac microvascular endothelial cells by suppressing TLR4/MAPK/NF-κB signaling. *42*(1), 505–513.
16. Han, Y., Yang, J., Fang, J., Zhou, Y., Candi, E., Wang, J.,.. . Shi, Y. (2022). The secretion profile of mesenchymal stem cells and potential applications in treating human diseases. Signal Transduct Target Ther, *7*(1), 92. doi:10.1038/s41392-022-00932-0
17. Huang, C., Meng, M., Li, S., Liu, S., Li, L., Su, Y.,.. . Biology, D. (2022). Umbilical Cord Mesenchymal Stem Cells Ameliorate Kidney Injury in MRL/lpr Mice Through the TGF-β1 Pathway. *10*.
18. Huang, M., Li, D., Chen, J., Ji, Y., Su, T., Chen, Y.,.. . therapy. (2022). Comparison of the treatment efficacy of umbilical mesenchymal stem cell transplantation via renal subcapsular and parenchymal routes in AKI-CKD mice. *13*(1), 1–11.
19. Huang, R., Liu, L., Li, B., Qin, L., Huang, L., Yeung, K. W.,.. . Technology. (2021). Nanograins on Ti-25Nb-3Mo-2Sn-3Zr alloy facilitate fabricating biological surface through dual-ion implantation to

concurrently modulate the osteogenic functions of mesenchymal stem cells and kill bacteria. *73*, 31–44.

20. International, F. J. K. (1992). Regeneration after acute tubular necrosis. *41*, 226–246.
21. Kholia, S., Sanchez, M., Cedrino, M., Papadimitriou, E., & Camussi, G. J. F. i. I. (2018). Human Liver Stem Cell-Derived Extracellular Vesicles Prevent Aristolochic Acid-Induced Kidney Fibrosis. *9*.
22. Lerman, L. O. J. T. i. M. M. (2021). Cell-based regenerative medicine for renovascular disease.
23. Li, H., Bai, G., Ge, Y., Zhang, Q., Kong, X., Meng, W., & Wang, H. (2018). Hydrogen-rich saline protects against small-scale liver ischemia-reperfusion injury by inhibiting endoplasmic reticulum stress. Life Sci, *194*, 7–14. doi:10.1016/j.lfs.2017.12.022
24. Lin, K. C., Yip, H. K., Shao, P. L., Wu, S. C., Chen, K. H., Chen, Y. T.,.. . Lee, M. S. (2016). Combination of adipose-derived mesenchymal stem cells (ADMSC) and ADMSC-derived exosomes for protecting kidney from acute ischemia-reperfusion injury. Int J Cardiol, *216*, 173–185. doi:10.1016/j.ijcard.2016.04.061
25. Ling, Jiang, Xue-Qi, Liu, Qiuying, Qin,.. . Biology, J.-N. J. F. j. o. p. o. t. F. o. A. S. f. E. (2018). hsa-miR-500a-3P alleviates kidney injury by targeting MLKL-mediated necroptosis in renal epithelial cells. fj201801711R.
26. Ling, Q., Yu, X., Wang, T., Wang, S.-G., Ye, Z.-Q., Liu, J.-H. J. C. P., & Biochemistry. (2017). Roles of the exogenous H2S-mediated SR-A signaling pathway in renal ischemia/reperfusion injury in regulating endoplasmic reticulum stress-induced autophagy in a rat model. *41*(6), 2461–2474.
27. Lu, T., Zhang, J., Cai, J., Xiao, J., Sui, X., Yuan, X.,.. . Lv, G. J. B. (2022). Extracellular vesicles derived from mesenchymal stromal cells as nanotherapeutics for liver ischaemia–reperfusion injury by transferring mitochondria to modulate the formation of neutrophil extracellular traps. *284*, 121486.
28. Martin, J. L., Gruszczyk, A. V., Beach, T. E., Murphy, M. P., & Saeb-Parsy, K. J. P. N. (2019). Mitochondrial mechanisms and therapeutics in ischaemia reperfusion injury. *34*(7), 1167–1174.
29. Matta, A., Karim, M. Z., Gerami, H., Benigno, B. Z., Cheng, I., Mehrkens, A., & Erwin, W. M. (2022). A Single Injection of NTG-101 Reduces the Expression of Pain-Related Neurotrophins in a Canine Model of Degenerative Disc Disease. Int J Mol Sci, *23*(10). doi:10.3390/ijms23105717
30. Nieuwland, R., Falcon-Perez, J. M., Thery, C., & Witwer, K. W. (2020). Rigor and standardization of extracellular vesicle research: Paving the road towards robustness. J Extracell Vesicles, *10*(2), e12037. doi:10.1002/jev2.12037
31. Paller, M. S., Hoidal, J. R., & Ferris, T. F. (1984). Oxygen free radicals in ischemic acute renal failure in the rat. J Clin Invest, *74*(4), 1156–1164. doi:10.1172/JCI111524
32. Panah, F., Ghorbanihaghjo, A., Argani, H., Zarmehri, M. A., & Ahmad, S. N. S. J. C. b. (2018). Ischemic acute kidney injury and klotho in renal transplantation. *55*, 3–8.
33. Pefanis, A., Ierino, F. L., Murphy, J. M., & Cowan, P. J. (2019). Regulated necrosis in kidney ischemia-reperfusion injury. Kidney Int, *96*(2), 291–301. doi:10.1016/j.kint.2019.02.009

34. Riazifar, M., Mohammadi, M. R., Pone, E. J., Yeri, A., Lasser, C., Segaliny, A. I.,.. . Hamamoto, A. J. A. n. (2019). Stem cell-derived exosomes as nanotherapeutics for autoimmune and neurodegenerative disorders. *13*(6), 6670–6688.
35. Su, L., Zhang, J., Gomez, H., Kellum, J. A., & Peng, Z. (2022). Mitochondria ROS and mitophagy in acute kidney injury. Autophagy, 1–14. doi:10.1080/15548627.2022.2084862
36. Yin, J., Chen, W., Ma, F., Lu, Z., Wu, R., Zhang, G.,.. . Wang, F. (2017). Sulodexide pretreatment attenuates renal ischemia-reperfusion injury in rats. Oncotarget, *8*(6), 9986–9995. doi:10.18632/oncotarget.14309
37. Zeid, A. S. S., Sayed, S. S. J. S. J. o. K. D., & Transplantation. (2020). A Comparative Study of the Use of Dexamethasone, N-acetyl Cysteine, and Theophylline to Ameliorate Renal Ischemia–Reperfusion Injury in Experimental Rat Models: A Biochemical and Immuno-histochemical Approach. *31*(5), 982.
38. Zhang, Y., Le, X., Zheng, S., Zhang, K., He, J., Liu, M.,.. . Therapy. (2022). MicroRNA-146a-5p-modified human umbilical cord mesenchymal stem cells enhance protection against diabetic nephropathy in rats through facilitating M2 macrophage polarization. *13*(1), 1–16.

Figures

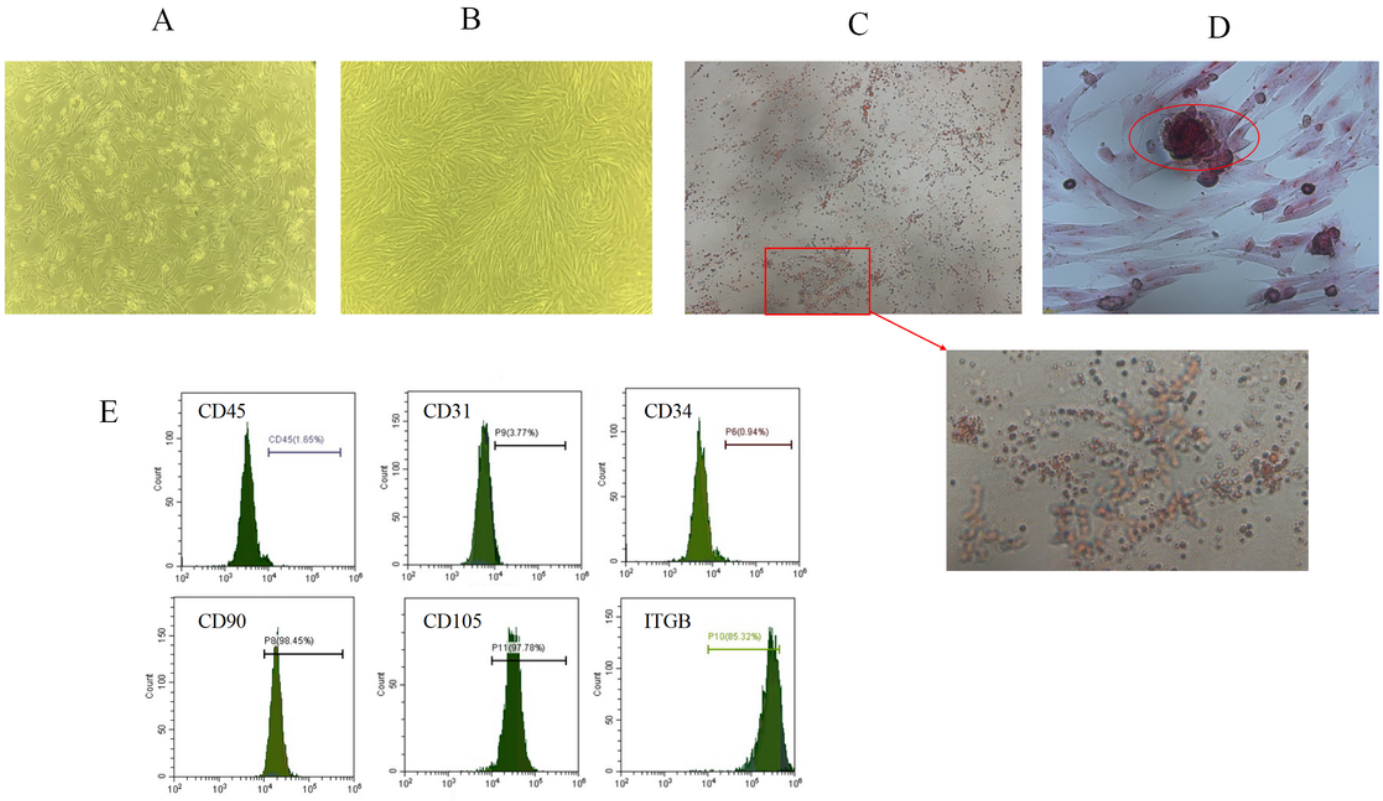

Figure 1

Characterization and Differentiation of ADMSC

(A) Morphology features of canine ADMSCs passage 0 and passage 3 (100×).

(B) Surface markers (CD34, CD29, CD45, CD105, ITGB and CD90) of ADMSCs (P3) detected by flow cytometry.

(C) ADMSC induced with osteogenic and lipogenic medium (100×).

Figure 2

Characterization of ADMSC-EVs

(A) ADMSC-EVs were observed via transmission electron microscopy and charactered as cup-shape with the diameter around 30-150 nm.

(B) Surface markers (CD9, CD63, TSG101) of ADMSC-EVs via western blot.

(C) The particle size distribution of EVs samples is shown by NTA analysis. The particle number of ADMSC-EVs suspension was 9.7×109/mL and the average particle size was 134 nm.

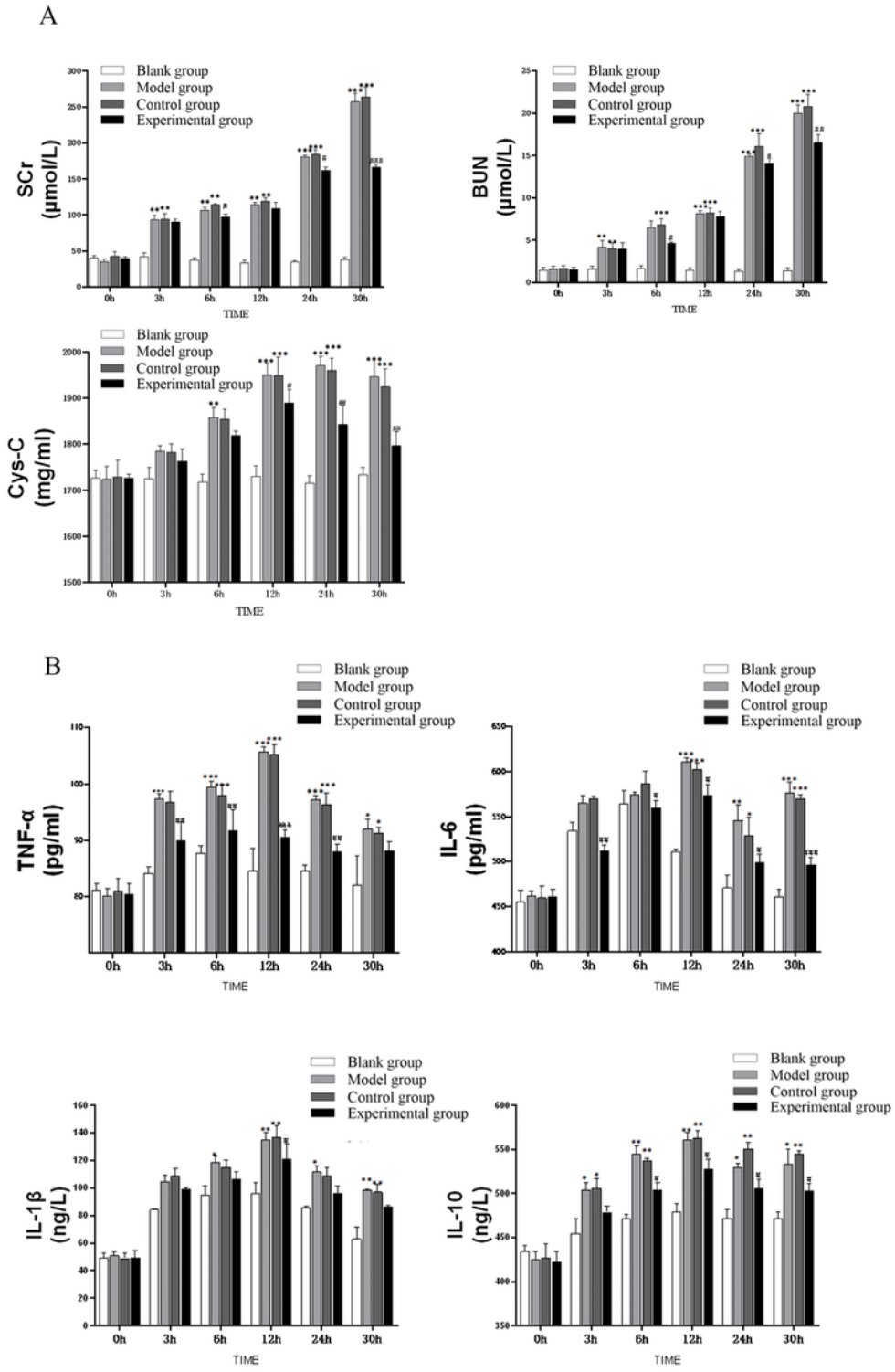

Figure 3

ADMSC-EVs protect renal IR from renal function (A) and Inflammatory reactions (A) in dogs (n = 5)

***p<0.01, **p<0.05, *p<0.1 vs. blank group, ###p<0.01, ##p<0.05, #p<0.1 vs. control group at the same time point.

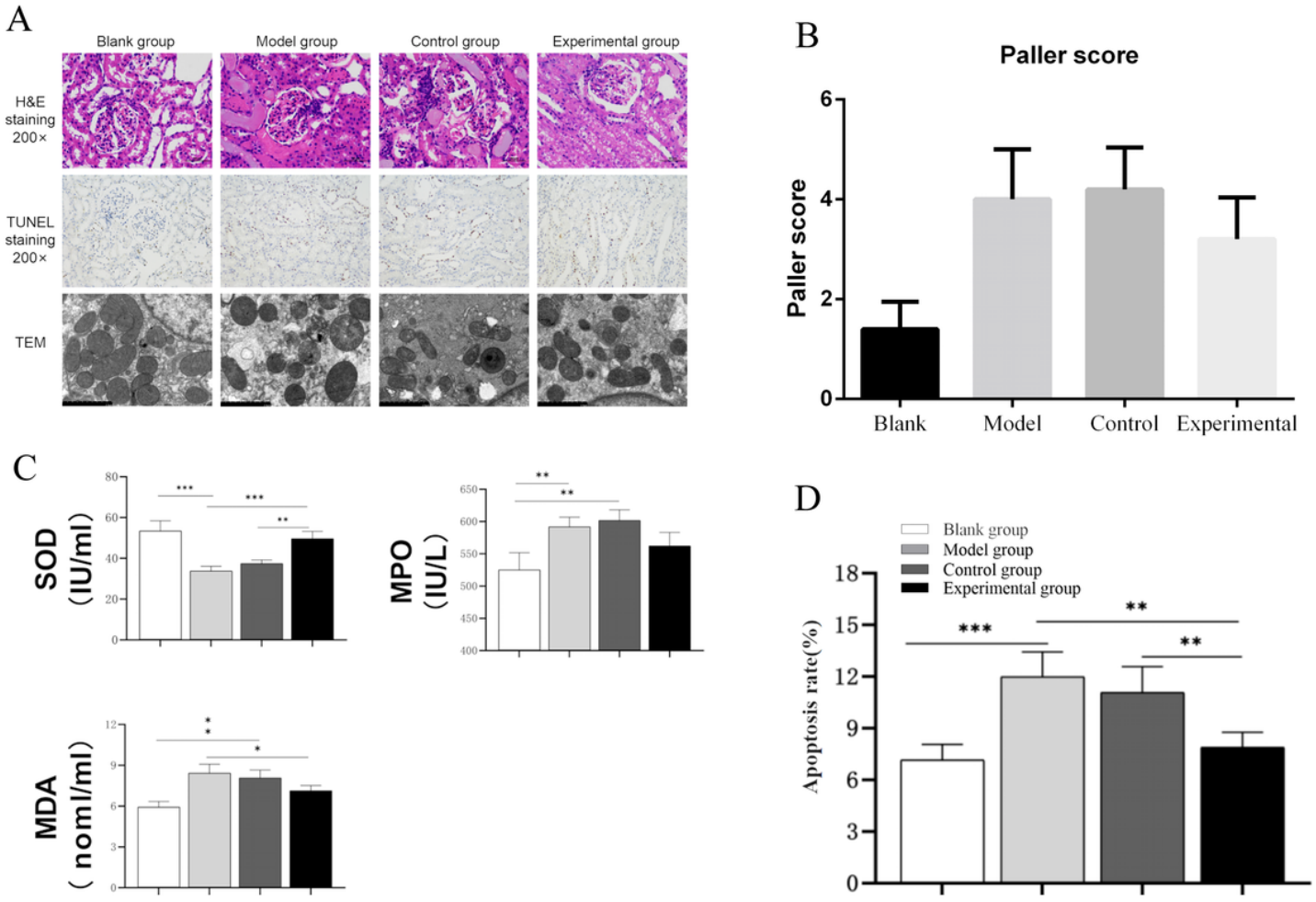

Figure 4

ADMSC-EVs protect renal IR from histological lesions (A, B), oxidative stress (C), mitochondrial damage (A) and cell apoptosis (A, D).

(A) Histological lesions, cell apoptosis and mitochondrial damage after 30h renal IR in dogs.

(B) Renal tubule injury evaluated by Paller scoring standard.

(C) Oxidative stress factors **after renal IR in dogs (n = 5)**

***p<0.01, **p<0.05, *p<0.1 vs. blank group, ###p<0.01, ##p<0.05, #p<0.1 vs. control group at the same time point.

(D) Apoptosis rate **after renal IR in dogs (n = 5)**

Positive rate = number of positive cells/total number of cells ×100%, ***p<0.01, **p<0.05.